Proc. of Workshop on Particle Distributions,
Chicago, IL, June 11-13,1998

BNL-65915

PX 169

CONF-9806135--

Presented at Workshop on Particle Distributions, Chicago, June 11-13,1998

SYSTEMATICS OF MID-RAPIDITY E_T AND MULTIPLICITY DISTRIBUTIONS IN NUCLEUS AND NUCLEON COLLISIONS AT AGS ENERGIES

M. J. TANNENBAUM, FOR THE E802 COLLABORATION
Brookhaven National Laboratory, Physics, Bldg. 510c, Upton, NY 11973-5000, USA
E-mail: mjt@bnl.gov

In the period 1986-1992, the E802 Collaboration at the BNL-AGS made systematic measurements of transverse energy (E_T) emission in an electromagnetic calorimeter (PbGl) which covered the pseudorapidity interval $1.25 \leq \eta \leq 2.50$ and half the azimuth (where mid-rapidity for these energies is $y_{cm}^{NN} \simeq 1.6 - 1.7$ depending the species). The other half of the azimuth was occupied by a 25 msr magnetic spectrometer with full particle identification. Runs were also taken with two different *full-azimuth* configurations of the PbGl, covering $1.25 \leq \eta \leq 2.44$, and also $1.3 \leq \eta \leq 2.4$. It was noticed[1] that the shapes of the upper edges of the E_T distributions, as represented for example by the p parameter in a gamma distribution fit, seemed to vary with the solid angle of the configuration. To systematically investigate this effect, the A-dependence and pseudorapidity-interval ($\delta\eta$) dependence of E_T distributions in the half-azimuth electromagnetic calorimeter were measured for p+Be, p+Au, O+Cu, Si+Au and Au+Au collisions.

1 E_T and Multiplicity distributions at mid-rapidity

The charged particle multiplicity, n, and its density in rapidity, dn/dy, are among the principal descriptive variables in both high energy and relativistic heavy ion physics. The rapidity regions of projectile and target fragmentation can be meaningfully discussed even at AGS energies. However, not until the c.m. energy, $\sqrt{s}$, reached $\sim$ 50 GeV (CERN ISR energies) so that the projectile and target rapidities are separated by $\sim \pm 4$ units could a clear mid-rapidity plateau of constant dn/dy spanning $\sim \pm 2$ units be discerned.[2]

The existence of the central plateau provided a stimulus for experimentalists to measure multiplicity distributions in a restricted pseudorapidity range, $|\eta - y_{cm}^{NN}| \leq 1.5$, "wide enough to allow for good statistics, yet sufficiently remote from the edge of the rapidity plateau to permit specific analysis of the central plateau."[2] Fowler and Weiner[3] emphasized that multiplicity distributions in small $\delta\eta$ intervals could be used as a tool to study hadron dynamics (coherence and correlations) since energy-momentum (and charge) constraints would not play a role as they do in full phase space measurements.

Transverse energy measurements in '4π' hadron calorimeters were intro-

duced [4] for the purpose of detecting and studying the hard-scattering of constituents of the proton (discovered at the CERN ISR via high p_T leading particles) by finding localized cores of energy deposition, 'jets', in an unbiased manner. However, the predominant source of transverse energy turned out to be the multiplicity weighted by the $<p_T>$ per particle, $dE_T/d\eta \sim <p_T> \times dn/d\eta$, so that the main utility of E_T distributions in nuclear collisions has been as an analog method of counting the multiplicity of relativistic particles emitted from a reaction to 'characterize' the 'nuclear geometry' (see Fig. 1).

1.1 'Centrality' and percentiles of E_T distributions

At the AGS, E802/E866 [1] and E814/E877 [5] use E_T in an electromagnetic [1] or hadronic [5] calorimeter to define 'centrality', typically by a certain upper percentile of the distribution (Fig. 1t). The upper tails of the less constrained distributions measured by E802/E866 in an EM calorimeter covering $1.3 \leq \eta \leq 2.4$ (and scaled by a factor of 4 in E_T for visual effect) fluctuate more (i.e. have a less steep upper edge) than the more constrained distributions measured by E814/E877 in a hadron calorimeter covering $0.83 \leq \eta \leq 4.7$, *but for the most part the distributions are very similar in shape, and therefore in centrality definition.* Note that for Au+Au, the E_T for a '4%' hard cut is $\sim$ 20% (!) below the 'knee' of the spectrum, while the E_T spectrum defined by the 4% zero degree calorimeter (ZCAL) cut spans a factor of ~ 2 in E_T.

1.2 Simple empirical models are instructive

The solid line shown on the E866 Au+Au spectrum is the result of an empirical 'Wounded projectile nucleon model (WPNM)' in which a B+A spectrum is composed of the sum of 1 to B-fold convolutions of the measured p+Au spectrum weighted according to the 'geometric' probability for 1, 2, ..., B of the projectile nucleons to interact in the target (see Figure 1b). [6] Figure 1b also shows the interesting feature at AGS beam energies that the maximum energy emission in ^{16}O+Cu is essentially the same as that in ^{16}O+Au. Furthermore, the high energy tails of the ^{16}O+Au and ^{16}O+Cu spectra are the same shape—the ratio of the cross sections at the highest energies becomes constant (a factor of ~ 6). This energy saturation is explained in the WPNM as the result of collisions in which all of the projectile nucleons interact—the constant ratio of the upper tails in ^{16}O+Cu collision compared to ^{16}O+Au is simply the geometrical ratio of the cross sections for all 16 projectile nucleons to interact in the respective targets.

DISCLAIMER

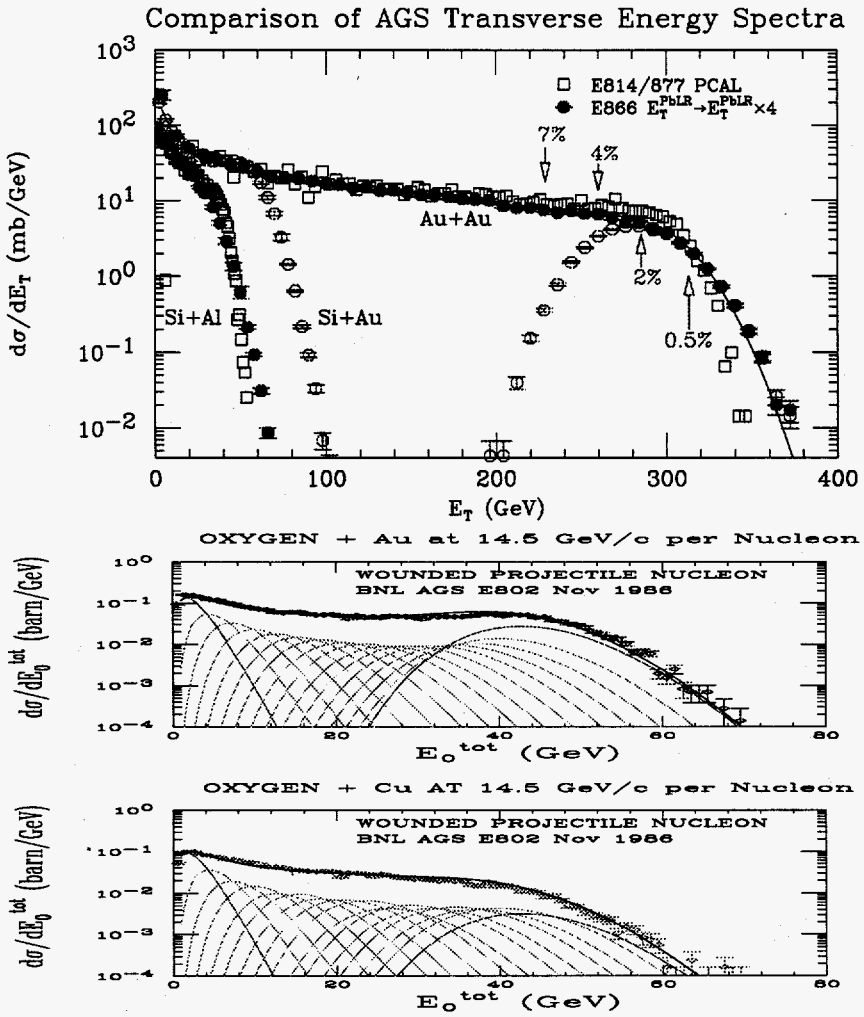

Figure 1: Top(t): E814/E877 E_T spectra in a full-azimuth hadron calorimeter compared to E802/E866 full azimuth E_T spectra in an EM calorimeter covering a smaller pseudorapidity interval. E802/E866 data include a central Au+Au spectrum defined by the 4 %-ile of the distribution in a Zero Degree Calorimeter (ZCAL). The solid line on the E802/E866 Au+Au data is an empirical calculation (see text). Bottom(b): Measured energy emission in E802 full azimuth EM calorimeter covering $1.25 \leq \eta \leq 2.44$ for ^{16}O+Au and ^{16}O+Cu reactions together with WPNM calculation; the individual components of the sum are also shown with the 1-fold and 16-fold p+Au convolutions emphasized.

1.3 Physics or acceptance?

It is also conceivable[7] that the saturation of the upper edges of the E802 E_T spectra at AGS energies could be an artifact of the limited angular (η) acceptance. In heavy ion collisions, the pseudorapdidity acceptance is an issue because naive models of successive collisions predict that the rapidity of the c.m. system, e.g. for a given projectile nucleon, shifts towards the target rapidity after each collision with a target nucleon—and vice-versa—such that the maximum in dn/dy and presumably $dE_T/d\eta$ moves towards the larger nucleus in an asymmetric B+A reaction. Therefore, an important issue to address is whether and how the pseudorapidity acceptance of E_T distributions affects the physical interpretion of the measurement. It is known[8] that the projectile dependence of a reaction is emphasized by measurements in the projectile fragmentation region, while the target dependence is emphasized by measurements in the target fragmentation region—thus, mid-rapidity measurements might represent a reasonable global average. An additional issue is whether the shapes of mid-rapidity E_T distributions change with the interval, $\delta\eta$.

2 The shapes of multiplicity distributions vs $\delta\eta$—'Intermittency'

It is well known, by now, that the shapes of multiplicity distributions for central collisions of relativistic heavy ions change with the size of the region of phase space in which they are measured—even for relatively 'small' changes of pseudorapidity interval in the range $0.1 \leq \delta\eta \leq 1.0$. This phenomenon, originally developed in terms of the normalized factorial moments of the multiplicity distributions and dubbed 'intermittency', has been explained by the dramatic reduction of the two-particle short-range rapidity correlation length ξ in central RHI collisions to a value, $\xi \sim 0.2$, which is much shorter than the value $\xi \sim 1-3$ in nucleon-nucleon collisions.[9]

The weakened, but finite, short-range rapidity correlations for central RHI collisions had been predicted: The chance of getting two hadrons from the same elementary collision decreases like the number of collisions, so the standard hadron short-range correlations vanish, but the quantum-mechanical Bose-Einstein correlations remain.[11,12] However, the fact that the *rapidity* correlation length from B-E interference is so short, $\xi_y = 0.19 \pm 0.03$, was not appreciated until demonstrated recently by E802,[13] in agreement with the multiplicity shape analysis.

The shapes of the charged multiplicity distributions (see Fig. 2) were well fit by Negative Binomial Distributions (NBD) and simply characterized by the NBD parameter $1/k(\delta\eta)$ which measures the additional fluctuation compared to a Poisson, where $\mu \equiv < n(\delta\eta) >$ is the mean multiplicity on the interval and

$\sigma \equiv \sqrt{< n^2 > - < n >^2}$ is the standard deviation:

$$\frac{\sigma^2}{\mu^2} = \frac{1}{\mu} + \frac{1}{k(\delta\eta)} \quad . \tag{1}$$

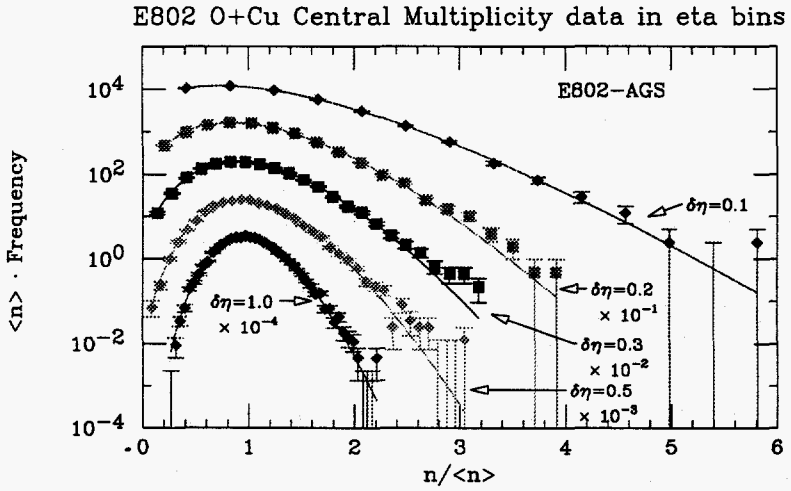

Figure 2: Multiplicity distributions measured in ^{16}O+Cu central collisions as a function of the interval $\delta\eta$ (indicated), scaled by $< n >$ on the interval, for the case when all 16 incident nucleons have interacted as determined by the ZCAL.

The shape of the charged multiplicity distribution varies from nearly exponential for $\delta\eta = 0.1$ to nearly gaussian for $\delta\eta = 1.0$. One assumes that the same effect, the variation in shape as a function of the pseudorapidity interval, $\delta\eta$, must occur with E_T distributions, but would likely be different in detail.

3 The 'Intermittency' Formalism

The study of non-Poisson fluctuations of charged particle multiplicity distributions in small pseudorapidity intervals $\delta\eta \leq 1$ by many experiments has been heavily influenced by the utilization of normalized factorial moments (NFM)

$$F_q(\delta\eta) = \frac{< n(n-1)\ldots(n-q+1) >}{< n >^q} \quad , \tag{2}$$

which are unity for a Poisson distribution.[14] The normalized factorial moment with the clearest interpretation is

$$F_2 = \frac{< n(n-1) >}{< n >^2} = \frac{< n^2 > - < n >}{< n >^2} = \frac{\sigma^2 + < n >^2 - < n >}{< n >^2}$$
$$= 1 + \frac{\sigma^2}{\mu^2} - \frac{1}{\mu} \quad . \tag{3}$$

The proposed[14] 'intermittency' phenomenon would be indicated by a power-law increase of multiplicity distribution NFM over pseudorapidity intervals ($\delta\eta$) as the size is reduced:

$$F_q(\delta\eta) \propto (\delta\eta)^{-\phi_q} \quad . \tag{4}$$

The scale-invariant power-law dependence with singular behavior as $\delta\eta \to 0$ was suggestive of the physics of phase transitions, fractals, and chaos.

Many experiments applied the formalism to their data, leading to the observation[14] of the predicted power law behavior in the region $1 \geq \delta\eta \geq 0.1$ (Fig. 3).[9] However, the observation of tantalizing power-laws tended to obscure the fact that multiplicity distributions were well known to be non-Poisson because of short-range rapidity correlations in multi-particle production.[10,11,12]

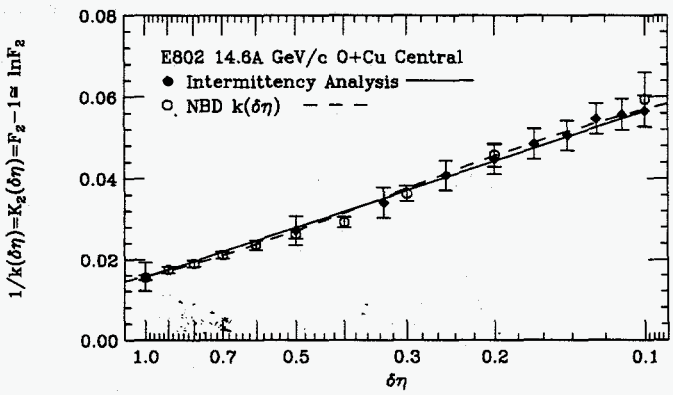

Figure 3: 'Log-Log' plot of $F_2(\delta\eta)$ for central (ZCAL) collisions of ^{16}O+Cu from E802 'Intermittency' analysis together with power-law fit (solid points, solid line). The open points are $1/k(\delta\eta)$ from the NBD fits of Fig. 2; the dashed line is Eq. 7.

4 Normalized Factorial Moments and Correlation Functions

It is important to understand that the q-fold normalized factorial moments for intermittency analyses are nothing other than averages of the q-particle short-range rapidity correlation functions on the interval $\delta\eta$. For instance, the $q = 2$ moment measures the weighted average of the normalized two-particle correlation function $R(y_1, y_2)$ on the interval $(0 \leq y_1, y_2 \leq \delta\eta)$:

$$F_2(\delta\eta) - 1 = K_2(\delta\eta) = \frac{\int^{\delta\eta} dy_1 dy_2\, \rho_1(y_1)\rho_1(y_2)R(y_1, y_2)}{\int^{\delta\eta} dy_1 dy_2\, \rho_1(y_1)\rho_1(y_2)} \quad , \qquad (5)$$

where K_2 is a normalized factorial cumulant [15]. $R(y_1, y_2)$ is the normalized two-particle correlation function from short-range rapidity correlation analyses which is typically parameterized as an exponential [11] :

$$R(y_1, y_2) = \frac{C_2(y_1, y_2)}{\rho_1(y_1)\rho_1(y_2)} = \frac{\rho_2(y_1, y_2)}{\rho_1(y_1)\rho_1(y_2)} - 1 = R(0,0)\, e^{-|y_1 - y_2|/\xi} \quad , \qquad (6)$$

where $\rho_1(y)$ and $\rho_2(y_1, y_2)$ are the inclusive densities for a single particle (at rapidity y) or 2 particles (at rapidities y_1 and y_2), $C_2(y_1, y_2) = \rho_2(y_1, y_2) - \rho_1(y_1)\rho_1(y_2)$ is the Mueller correlation function for 2 particles (which is zero for the case of no correlation), [10] and ξ is the two-particle short-range rapidity correlation length. The relationship between the intermittency formalism and the two-particle correlation becomes clear when $\rho_1(y) = dn/dy$ is constant on the interval, in which case: [3]

$$K_2(\delta\eta) = F_2(\delta\eta) - 1 = R(0,0) \left\{ 2\, \frac{(x - 1 + e^{-x})}{x^2} \right\} \quad , \qquad (7)$$

where the quantity in braces is a function, denoted $G(x)$, of the scaled variable $x \equiv \delta\eta/\xi$. For a NBD: $K_2(\delta\eta) = 1/k(\delta\eta)$ and the $K_q = (q-1)!\, K_2^{q-1}$ are all determined by the single parameter $k(\delta\eta)$.

The NBD approach made it clear that singularities are difficult to plot—even on log paper. Instead of plotting $K_2(\delta\eta) = 1/k(\delta\eta)$ to see a divergence as $\delta\eta \to 0$, it is preferable to plot $k(\delta\eta) = 1/K_2(\delta\eta)$ to see whether $k(0) \to 0$. In fact, all measurements of NBD fits (see Fig. 4) show roughly linear $k(\delta\eta)$ with non-zero intercept $k(0) \neq 0$—therefore, no singularity. [11,12]

5 Systematics of Mid-rapidity E_T distributions

Recently, E_T measurements in limited solid angle have become quite popular as a definition 'centrality' in RHI collisions. Hence, it seemed worthwhile to in-

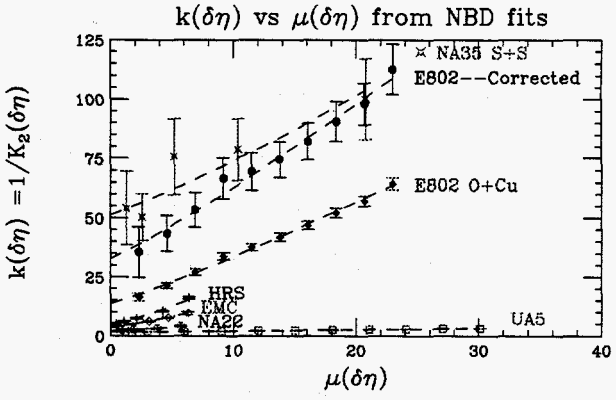

Figure 4: $k(\delta\eta)$ as a function of the mean multiplicity in the interval, $\mu(\delta\eta) = dn/d\eta \times \delta\eta$ for several experiments: UA5 $\bar{p}$+p, NA22 p+p, EMC μ-p, HRS $e^+ + e^-$, E802 O+Cu central (and E802 corrected), NA35 S+S central. The dashed lines are fits to Eq. 7.

vestigate how small a $\delta\eta$ interval would still give a meaningful characterization of the 'nuclear geometry' of a reaction. Also, as noted above, simple models have proved useful in understanding the detailed shape of E_T distributions in B+A collisions as a sum of independent collisions weighted according to the 'geometric' probability of the number of total (WNM) or projectile (WPNM) participants in the reaction. If the 'shape' of E_T distributions were controlled by a correlation length and strength which changed with the number of participants *differently* from the effect of random combinations, then these simple models would make no sense, and, in particular, would fail to reproduce the shapes of the upper edges of the spectra.

Systematic measurements of the A dependence of mid-rapidity E_T distributions as a function of the $\delta\eta$ interval were made using the E802 electromagnetic calorimeter (PbGl) which covered half the azimuth with a pseudorapidity acceptance $1.25 \leq \eta \leq 2.50$ (where mid-rapidity for these energies is $y_{cm}^{NN} \simeq 1.6 - 1.7$ depending the species). The pseudorapidity distributions, $dE_T/d\eta$ for fixed E_T, have already been published. [16,1] In the present study, the η-acceptance of the calorimeter, $1.25 \leq \eta \leq 2.50$, is subdivided into 8 nominally equal bins of 0.16 in pseudorapidity, i.e. $1.22 \leq \eta \leq 1.38$, $1.38 \leq \eta \leq 1.54$, $\ldots 2.34 \leq \eta \leq 2.50$. The acceptance ($\Delta\eta \times \Delta\phi$) of each bin varies compared to the ideal $0.16 \times \pi$, but no correction has been made here for this effect. The E_T distributions (in $\Delta\phi = \pi$) are then measured for successively smaller $\delta\eta$ intervals centered (except for the smallest) on $\eta|_0 = 1.86$: $\delta\eta = 1.28$, the full η-acceptance of the calorimeter (actually $1.25 \leq \eta \leq 2.50$); $\delta\eta = 0.96$

$(1.38 \leq \eta \leq 2.34)$; $\delta\eta = 0.64$ $(1.54 \leq \eta \leq 2.18)$; $\delta\eta = 0.32$ $(1.70 \leq \eta \leq 2.02)$; $\delta\eta = 0.16$ $(1.70 \leq \eta \leq 1.86)$. The results for ^{16}O+Cu and for ^{197}Au+Au are shown in in Fig. 5. Evidently, the shapes of the upper edges of E_T distributions change with $\delta\eta$, similarly to Fig. 2.

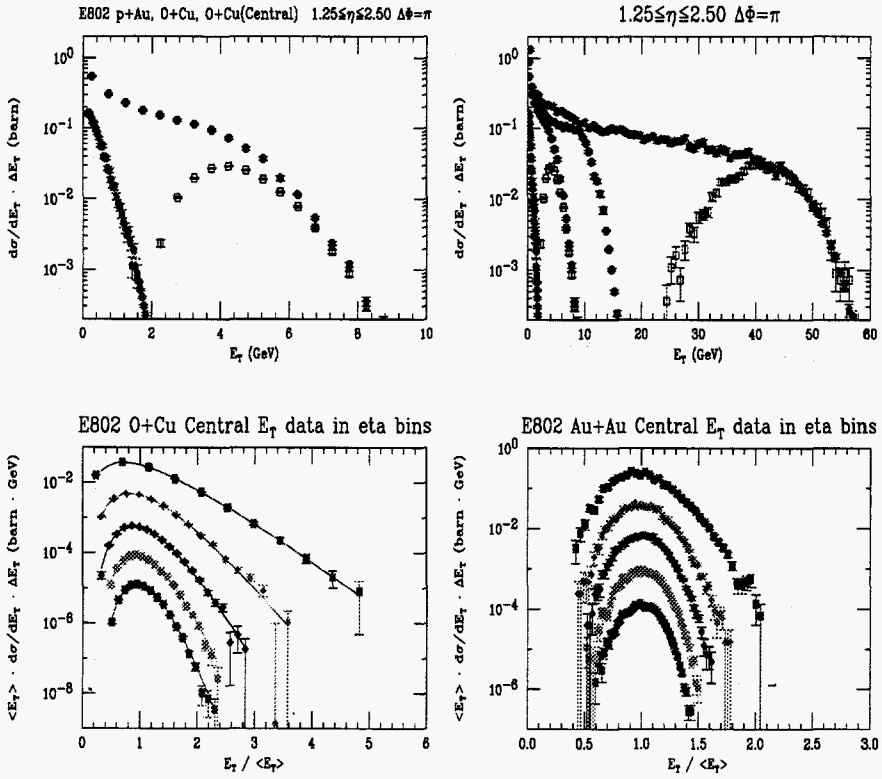

Figure 5: Top: E802 mid-rapidity E_T distributions $(\Delta\phi = \pi)$ for the interval $1.25 \leq \eta \leq 2.50$. (Left) p+Au, O+Cu, O+Cu(ZCAL); (Right) previous data, plus Si+Au, Au+Au, Au+Au(ZCAL). Bottom: Central (ZCAL) E_T distributions as a function of $\delta\eta$, normalized by $< E_T >$ on the interval. O+Cu (left), Au+Au (right).

6 Is the WPNM preserved as a function of $\delta\eta$?

In order to perform a WPNM calculation as a function of $\delta\eta$, the E_T distributions of p+Au and p+Be were obtained as a function of $\delta\eta$ as above (see Fig. 6). The original E802 measurements [6,16] in the full η-acceptance of the

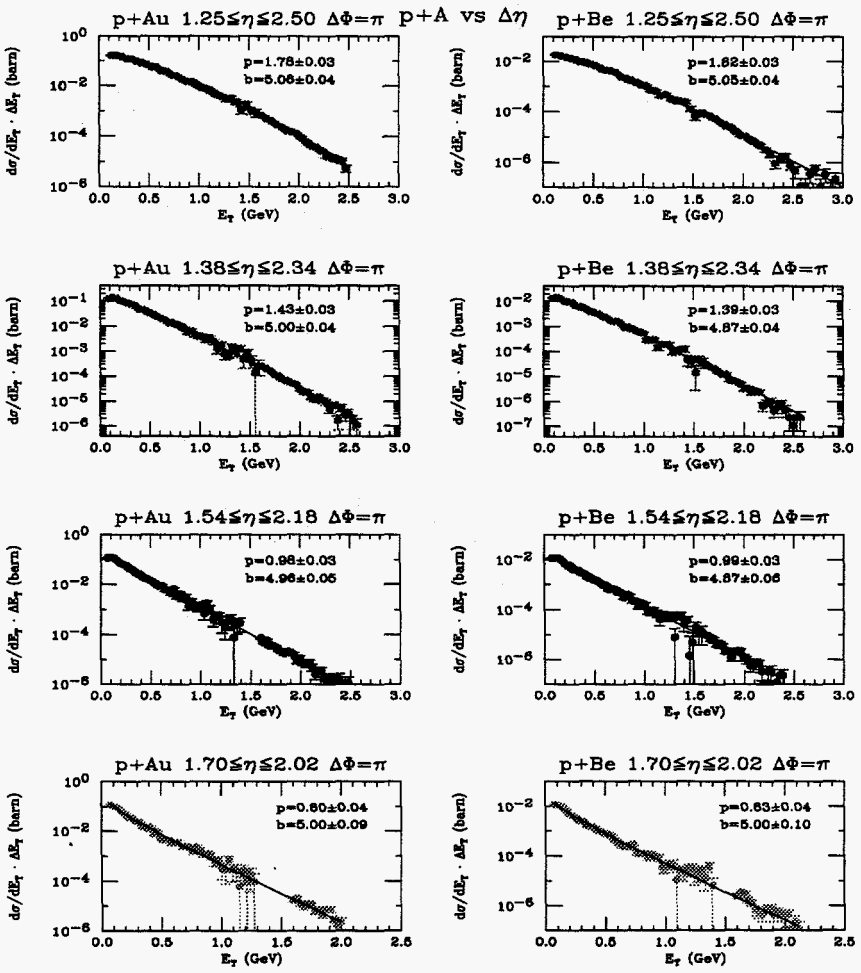

Figure 6: E_T distributions for p+Au (left) and p+Be (right) as a function of decreasing $\delta\eta$ from top to bottom. Adjacent p+Au and p+Be plots have the same $\delta\eta$.

calorimeter showed that the mid-rapidity E_T spectra of p+Au, p+Cu, p+Al and p+Be all exhibit the same shape over roughly 5 decades of cross section—no obvious multiple collisions effects were evident at mid-rapidity for p+A at AGS energies. In the present measurement, as the $\delta\eta$ interval is reduced, the shapes of the E_T spectra clearly change with $\delta\eta$ for both p+Au and p+Be; but in each $\delta\eta$ interval, the shapes of the p+Au and p+Be distributions remain

essentially *identical* with each other. This striking effect is exhibited quantitatively by the equality of the Γ-distribution fit parameters b and p in each interval as shown on Fig. 6. Figure 7 shows that the WPNM calculations for O+Cu, Si+Au, Au+Au continue to work well as $\delta\eta$ is reduced.

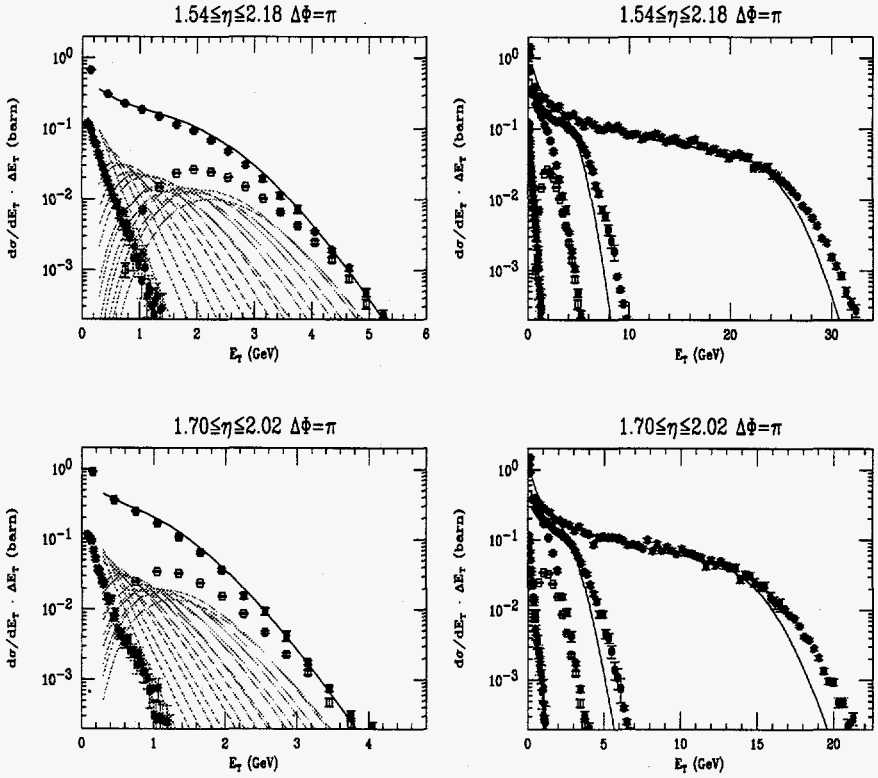

Figure 7: WPNM calculations (lines) for the two smallest $\delta\eta$ intervals for (left) O+Cu, (right) Si+Au, Au+Au. Components are shown for O+Cu. Data shown are (left) p+Au, O+Cu, O+Cu (ZCAL); (right) same data plus Si+Au, Au+Au.

The WPNM calculation for B+A reaction is given by the sum:

$$\left(\frac{d\sigma}{dE_T}\right)_{\mathrm{WPNM}} = \sigma \sum_{n=1}^{B} w_n \, P_n(E_T) \tag{8}$$

where σ is the measured B+A cross section in the interval $\delta\eta$, w_n is the relative probability for n projectile participants in the B+A reaction and $P_n(E_T)$ is the

calculated E_T distribution on the $\delta\eta$ interval for n independently interacting projectile nucleons. If $f_1(E_T)$ is the measured E_T spectrum in the $\delta\eta$ interval for one projectile nucleon, in this case the p+Au spectrum, and p_0 is the probability for a p+Au collision to produce no signal in the $\delta\eta$ interval, then $P_n(E_T)$ (including the p_0 effect) is

$$P_n(E_T) = \sum_{i=0}^{n} \frac{n!}{(n-i)!\ i!}\, p_0^{n-i}(1-p_0)^i f_i(E_T) \tag{9}$$

where $f_i(E_T)$ is the i-th convolution of $f_1(E_T)$. Since the p+Au data in each $\delta\eta$ interval are nicely fit by Γ-distributions

$$f_1(x) = \frac{b}{\Gamma(p)}(bx)^{p-1}e^{-bx} \quad , \tag{10}$$

the convolution is simple: for $f_i(E_T)$, $p \to i \times p$ while b remains unchanged. As smaller and smaller $\delta\eta$ intervals are used for the E_T spectra, the probability p_0 for a p+Au reaction to produce zero signal on the interval becomes larger and larger. This effect is easily measured from the ratio of detected cross section in the $\delta\eta$ interval to the inelastic p+Au cross section of 1662mb, and must be taken into account when performing the WPNM.[16] The values of p_0 are 0.08, 0.16, 0.33, 0.33 for the $\delta\eta$ intervals of Fig. 6.

7 Comparison E802 of $dn/dy|_{\pi^+}$ and E_T in A+A collisions

On Fig. 8, the $dn/dy|_{\pi^+}$ distributions for p+A inclusive and A+A central are compared to the E_T distributions of Fig. 5t (with Si+Al in place of O+Cu). The A dependence of "produced particles" (represented by identified π^+) at mid-rapidity clearly tracks the mid-rapidity E_T distributions very well. The comparison Au+Au/Si+Al is intriguing since the Au+Au/Si+Al data for both dn/dy and E_T are close to the ratio of 7 (predicted by the Wounded Nucleon Model). However, from the E_T distributions, it is obvious that the exact value of this ratio (also, for the π^+ data) depends on the "centrality" cut used, since the "shapes" of the distributions vary with A. The p-p, p+Be and p+Au data for π^+ support the mid-rapidity E_T result of no multiple collision effect since $dn/dy|_{\pi^+}$ is the same for all three reactions at mid-rapidity while there are clear differences in the beam and target fragmentation regions.

8 CONCLUSIONS

1. The shapes of E_T distributions change with $\delta\eta$ interval.

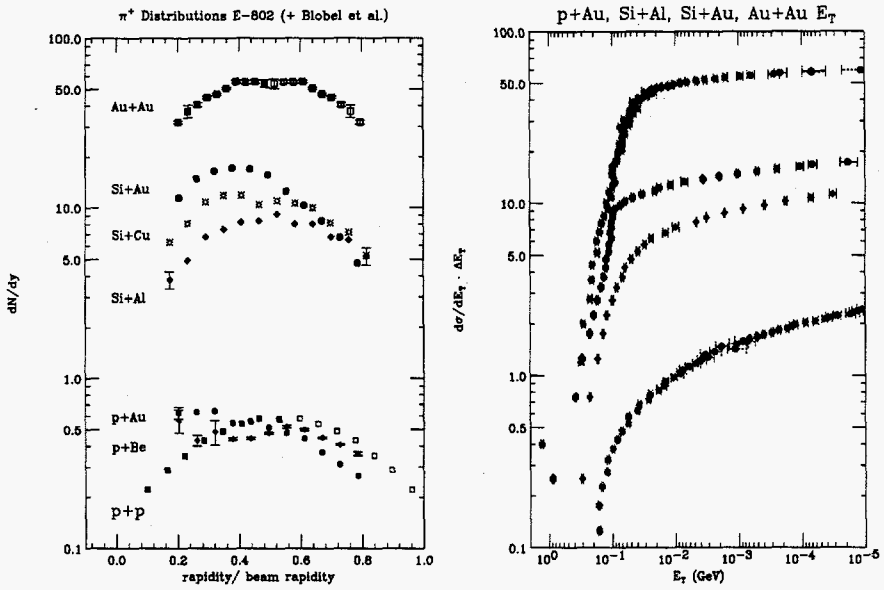

Figure 8: Comparison of E802 $dn/dy|_{\pi^+}$ (left) to mid-rapidity E_T (right) distritubions.

2. The shape $\Gamma(p, b)$ and change of shape with $\delta\eta$ is **Identical** for p+Au and p+Be in E802 for $0.2 \leq \delta\eta \leq 1.25$, around mid-rapidity.

3. The shape (or fluctuation) of multiplicity distributions as parameterized by Normalized Factorial Moments or the NBD parameter $1/k = K_2$ can be related to 2-particle correlations by an elegant theoretical framework; but we could find no such framework for the Gamma Distribution parameter $p(\delta\eta)$ nor for E_T correlations.

4. The Wounded Projectile Nucleon model works remarkably well to relate all the measured spectral shapes of Electromagnetic E_T distributions from p+Au, to O+Cu, to Si+Au to Au+Au at AGS energies for pseudorapidity intervals $\delta\eta$ in the range $0.2 \leq \delta\eta \leq 1.25$.

5. It is clear that E_T distributions in limited regions of $\delta\eta$ provide an excellent characterization of the 'nuclear geometry' of RHI collisions, from which important information about the dynamics can be inferred.

6. At AGS energies, the overall production of particles as observed by mid-rapidity E_T distributions may be interpreted as arising from incoherent

nucleon-nucleus collisions, with the further implication that the stopping of the participant nucleons observed in central Au+Au collisions must be related to the identical shapes and evolution of the E_T distributions for p+Au and p+Be. In other words, the 'stopping' should be observable in p+A 'central' collisions.

Acknowledgments

This paper has been authored under contract number DE-AC02-98CH10886 with the U.S. Department of Energy. Accordingly, the U.S. Government retains a non-exclusive, royalty-free license to publish or reproduce the published form of this contribution, or allow others to do so, for U.S. Government purposes.

References

1. L. Ahle, *et al*, E802 Collaboration, *Phys. Lett.* B **332**, 258 (1994)
2. W. Thomé, *et al*, *Nucl. Phys.* B **129**, 365 (1977)
3. G. N. Fowler and R. M. Weiner, *Phys. Lett.* B **70**, 201 (1977)
4. J. D. Bjorken, *Phys. Rev.* D **8**, 4098 (1973)
5. J. Barrette, *et al*, E814/E877 Collaboration, *Phys. Rev. Lett.* **70**, 2996 (1993)
6. T. Abbott, *et al*, E802 Collaboration, *Z. Phys.* C **38**, 35 (1988)
7. R. Albrecht, *et al*, WA80 Collaboration, *Z. Phys.* C **38**, 3 (1988)
8. e.g. see M. J. Tannnenbaum, *Nucl. Phys.* A **488**, 555c (1988)
9. T. Abbott, *et al*, E802 Collaboration, *Phys. Rev.* C **52**, 2663 (1995)
10. A. H. Mueller, *Phys. Rev.* D **4**, 150 (1971)
11. Detailed citations are not reasonable here. See the following reference [12] for more complete citations.
12. M. J. Tannenbaum, *Phys. Lett.* B **347**, 431 (1995)
13. Y. Akiba, *et al*, E802 Collaboration, *Phys. Rev.* C **56**, 1544 (1997)
14. For an extensive review of this work, see A. Bialas, *Nucl. Phys.* A **525**, 345c (1991)
15. The normalized factorial cumulants, K_q, which are zero if there is no direct q particle correlation (Poisson distribution), are just the normalized factorial moments, F_q, with all q-fold combinations of lower order correlations subtracted [10]: $K_2 = F_2 - 1$, $K_3 = F_3 - (1 + 3K_2)$, $K_4 = F_4 - (1 + 6K_2 + 3K_2^2 + 4K_3) \ldots$
16. T. Abbott, *et al*, E802 Collaboration, *Phys. Rev.* C **45**, 2933 (1992)